Applied Mathematics & Information Sciences
An International Journal

http://dx.doi.org/10.12785/amis/090242

Thrust for Permanent Magnet Linear Synchronous Motor

Hengkun Liu[*] *and Hu Cheng*

College of Mechatronics Engineering and Automation, National University of Defense Technology, ChangSha, Hunan 410073, China

Received: 13 Jun. 2014, Revised: 11 Sep. 2014, Accepted: 13 Sep. 2014
Published online: 1 Mar. 2015

Abstract: In order to increase the traction efficiency and driving speed of low-speed maglev train, synchronous traction technology is applied to low-speed maglev train. In order to reduce the normal force of the motor and enhance the stationarity of traction, the motor is designed with air-core coil as primary and permanent magnet Halbach array as secondary. Through theoretical analysis, the analytical expression of motor thrust and normal force is concluded and the thrust of motor is measured on the basis of a certain permanent magnet linear synchronous motor test platform. The effectiveness of the analytical method is verified by means of the measurement result accordingly.

Keywords: linear synchronous motor, permanent magnet Halbach array, D-H conversion, thrust of motor

1 Preface

Maglev train is arousing more and more concerns by virtue of its intrinsic advantages. As the low-speed maglev train is restricted by eddy current effect, the problem of low train traction efficiency and running speed is found [1]. In order to remedy such defect, this article introduces permanent magnet linear synchronous motor (PMLSM) into low-speed maglev train. The PMLSM composed of air-core coil (ILC) and permanent magnet Halbach array (PMH). As secondary of motor, PMH is advantaged by simple structure, passive energy-saving, etc, by making use of permanent magnets to generate magnetic fields [2]. In addition, Halbach array strengthens obviously the magnetic fields on one of its sides distributing in approximate sine and on the other side distributing in zero, and thus the effect of the permanent magnetic fields gives full play [3]. As primary of motor, ILC overcomes the problem that the iron core of the coil produces normal force. If the power angle between the primary and the secondary is controlled reasonably, it will achieve the effect that the motor's normal force is zero in event of maximal thrust [4].

The analytical method and the finite element method are two main methods which are applied to calculate the thrust of motor.

The physical concept of the analytical method is clear. This method can be directly used for analysis and design, and can be applied to guide optimization and characteristics. Lu Qinfen[5] uses the equivalent circuit method, calculate the effective air-gap, armature, excitation of LSM motor parameters, and derive analytical expression of motor's thrust. Based on the flux equation, Pang Hongshuai[6] obtained the mathematical model of linear synchronous motor. The model is used to simulate the motor start and steady process. Qiu Lin[7] used the equivalent magnetic permeability and equivalent current layer concept, obtained the simplified hierarchical model of linear motor. By solving the Maxwell equation model, the expression of propulsive force and normal force is obtained. By using the Maxwell tensor method, Li Chengjun[8] obtained the mathematical model of the electromagnetic force of permanent magnet linear synchronous motor.

With the development of finite element analysis software, the finite element method is widely used in motor analysis. By using finite element software, Hu Ganjuan[9] analyzed the levitation field and propulsion field of LSM, gives the motor force with excitation current, and obtained the relation between the thrust and current, power angle, the height of the air-gap, slot. Sun Peng[10], by using finite element method, analyzed the air-gap magnetic field of the permanent magnetic linear synchronous motor.

At present, motor composed of Halbach array and air-core coil, only applied in American GA maglev system[11,12] and Magplane company's pipeline transportation systems[13,14]. Zhang Yong[15] proposed

[*] Corresponding author e-mail: liberry@sina.com

a motor structure composed of air core coil and permanent magnet, expressions are derived for the magnetic field and the force motor. To the permanent magnet linear Halbach array, James F. Hoburg[16] obtained the distribution of the magnetic field of arbitrary magnetization angle permanent magnet. The results are not used to guide the design of linear motor structure. By using he magnetization vector method, Z. P. Xia[17], obtained the distribution of internal, external magnetic field about ring permanent magnet motors Halbach array. When the radius of the motor is large enough, the results can be extended to compute linear Halbach array permanent magnet magnetic field.

In these studies, there is no literature about the LSM motor composed of permanent magnet Halbach array and air core coil. In this paper, analytic calculation method for the air-gap magnetic field and thrust is studied.

1. Permanent Magnet Halbach Structure

In August 1978, K. Halbach, an American physicist, proposed a novel permanent magnet structure [18] called as permanent magnet Halbach array (PMH) as seen in Fig. 1.

That is quite beneficial to increasing torque density and power density of motor [19,20].

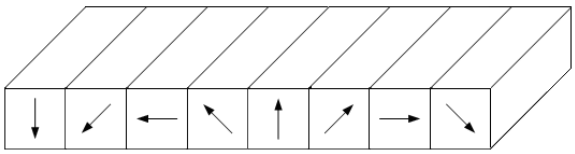

Fig. 1: Halbach Permanent Magnet Structure

2 Calculation of Motor Thrust

2.1 Calculation of surface current

Suppose the permanent magnet is infinitely long in the X direction (direction of motor width). The magnetic fields as generated by it are in the YZ plane as seen in Fig. 2.

The magnetic fields of permanent magnet segment equal to the sum of vectors of the magnetic fields generated by all the surface current[21].

As shown in Fig. 3, from the right hand rule, the four surface current of permanent magnet segment are:

$$\begin{aligned} I_1 &= \quad 2a \cdot H_c \cdot \sin\alpha, I_2 = \quad 2b \cdot H_c \cdot \cos\alpha \\ I_3 &= -2a \cdot H_c \cdot \sin\alpha, I_4 = -2b \cdot H_c \cdot \cos\alpha \end{aligned} \tag{1}$$

2.2 Calculation of plane magnetic fields

Fig. 4 is the schematic diagram of single surface current composed of infinitely long positive current

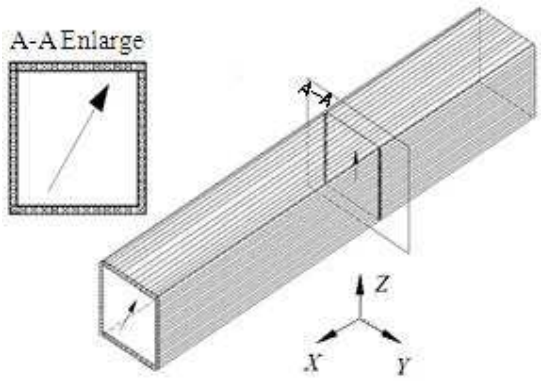

Fig. 2: Plane Field of Permanent Magnet Segments

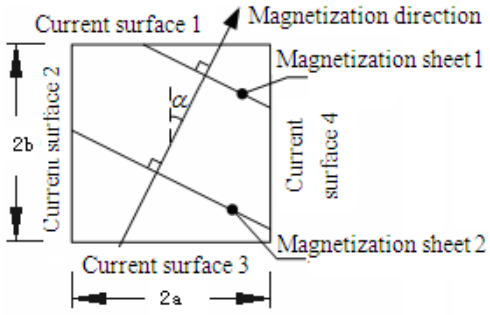

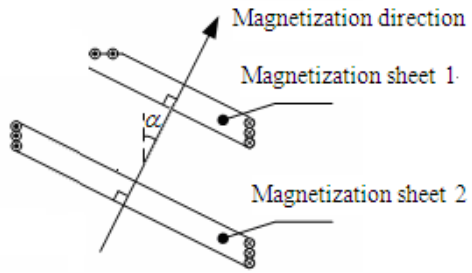

Fig. 3: Permanent magnet segments

elements. According to the Ampere circuital theorem, the magnetic field in Point (y_0, z_0) is:

$$dB_0 = \left(\mu_0 I / 4\pi l R\right) dz \tag{2}$$

The magnetic field in the directions of y and z are:

$$\begin{aligned} dB_{y0} &= \frac{\mu_0 I}{4\pi \cdot l} \cdot \frac{z - z_0}{{y_0}^2 + (z_0 - z)^2} \cdot dz \\ dB_{z0} &= \frac{\mu_0 I}{4\pi \cdot l} \cdot \frac{y_0}{{y_0}^2 + (z_0 - z)^2} \cdot dz \end{aligned} \tag{3}$$

The magnetic field is integral of all elementary current magnetic fields as shown in Figure 4. The magnetic field

generated by the surface at Point (y_0, z_0) is:

$$B_{y0} = \frac{\mu_0 I}{8\pi \cdot l} \cdot \ln \frac{y_0^2 + (z_0 - l)^2}{y_0^2 + (z_0 + l)^2}$$
$$B_{z0} = \frac{\mu_0 I}{4\pi \cdot l} \cdot \left[\arctan \frac{z_0 + l}{y_0} - \arctan z_0 - l y_0 \right] \quad (4)$$

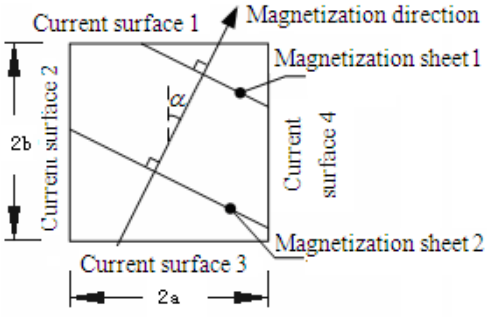

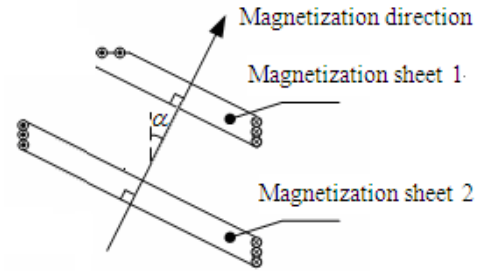

Fig. 4: Single surface current

2.3 Calculation of magnetic fields

The permanent magnet segment as shown in Figure 5. Define global coordinate system $\{S\}$ in Figure 5. And define local coordinate system $\{S_k\}(k = 1,2,3,4)$ on each of the current surfaces, then the homogeneous transformation matrix[22] of each surface current coordinate system relative to $\{S\}$ are respectively:

$$T_1 = \left[\begin{array}{c|c} R_1 & \begin{matrix} 0 \\ b \end{matrix} \\ \hline \begin{matrix} 0 & 0 \end{matrix} & 1 \end{array}\right], T_2 = \left[\begin{array}{c|c} R_2 & \begin{matrix} -a \\ 0 \end{matrix} \\ \hline \begin{matrix} 0 & 0 \end{matrix} & 1 \end{array}\right],$$
$$T_3 = \left[\begin{array}{c|c} R_3 & \begin{matrix} 0 \\ -b \end{matrix} \\ \hline \begin{matrix} 0 & 0 \end{matrix} & 1 \end{array}\right], T_4 = \left[\begin{array}{c|c} R_4 & \begin{matrix} a \\ 0 \end{matrix} \\ \hline \begin{matrix} 0 & 0 \end{matrix} & 1 \end{array}\right] \quad (5)$$

In which

$$R_1 = \begin{bmatrix} 0 & 1 \\ -1 & 0 \end{bmatrix}, R_2 = \begin{bmatrix} 1 & 0 \\ 0 & 1 \end{bmatrix},$$
$$R_3 = \begin{bmatrix} 0 & 1 \\ -1 & 0 \end{bmatrix}, R_4 = \begin{bmatrix} 1 & 0 \\ 0 & 1 \end{bmatrix} \quad (6)$$

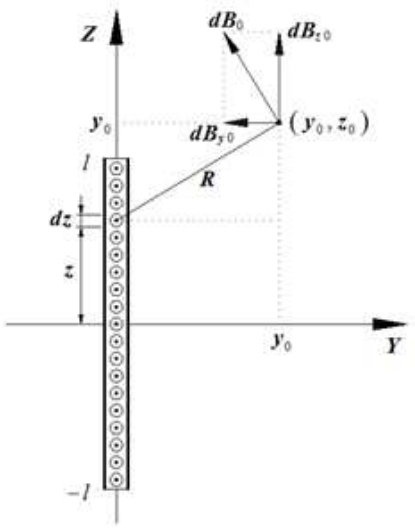

Fig. 5: Coordinate System of Permanent Magnet Segments

Suppose the coordinate of any point P in $\{S\}$ is $\begin{bmatrix} y & z \end{bmatrix}^T$. The coordinate $\begin{bmatrix} y_k & z_k \end{bmatrix}^T$ of Point P in $\{S_k\}$ can be solved from the following formula:

$$\begin{bmatrix} y_k & z_k & 1 \end{bmatrix} = \begin{bmatrix} y & z & 1 \end{bmatrix} \cdot \left(T_k^{-1}\right)^T \quad (7)$$

Substituting (1) and (7) into (4), the expression of magnetic fields can be obtained:

$$\begin{bmatrix} B_y \\ B_z \end{bmatrix} = \sum_{k=1}^{4} R_k \cdot \begin{bmatrix} B_{yk} \\ B_{zk} \end{bmatrix} \quad (8)$$

Then the magnetic field as follows:

$$B_y = \frac{\mu_0 H_c \cdot \cos\alpha}{4\pi} \cdot \ln \left[\frac{(y+a)^2 + (z-b)^2}{(y+a)^2 + (z+b)^2} \cdot \frac{(y-a)^2 + (z+b)^2}{(y-a)^2 + (z-b)^2} \right] + \frac{\mu_0 H_c \cdot \sin\alpha}{2\pi} \cdot \left(\arctan \frac{y+a}{z+b} + \arctan \frac{y-a}{z-b} - \arctan \frac{y+a}{z-b} - \arctan \frac{y-a}{z+b} \right) \quad (9)$$

$$B_z = \frac{\mu_0 H_c \cdot \sin\alpha}{4\pi} \cdot \ln \left[\frac{(y+a)^2 + (z-b)^2}{(y-a)^2 + (z-b)^2} \cdot \frac{(y-a)^2 + (z+b)^2}{(y+a)^2 + (z+b)^2} \right] + \frac{\mu_0 H_c \cdot \cos\alpha}{2\pi} \cdot \left(\arctan \frac{z+b}{y+a} + \arctan \frac{z-b}{y-a} - \arctan \frac{z-b}{y+a} - \arctan \frac{z+b}{y-a} \right) \quad (10)$$

The positive directions of B_y and B_z in Formula (9) and (10) are the same as those in Axis Y and Axis Z.

2.4 Analytical solution of magnetic field

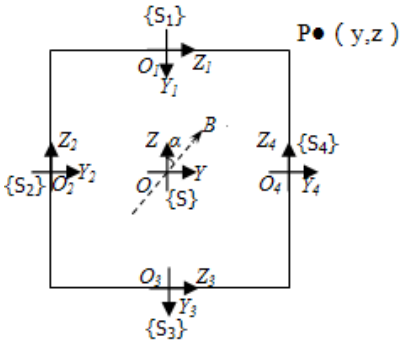

Fig. 6: Coordinate System of PMH Array

For PMH array as shown in Figure 6, suppose the number of segments is n, the magnetization angle of the first permanent magnet segment is α_0 and then increasing by $\Delta\alpha$ progressively in turn. Then the magnetic fields generated by the whole Halbach array in the figure can be calculated according to the following steps.

According to the supposition, it can be known that the magnetization angle of No.k permanent magnet in PMH array is:

$$\alpha_k = \alpha_0 + (k-1)\cdot\Delta\alpha \tag{11}$$

By reference to the coordinate system $\{S\}$ as shown in Figure 5, build body coordinate system $\{S_k\}\,(k=1,\cdots,n)$ on No.k permanent magnet and set the base coordinates $\{0\}$ and $\{1\}$ of the whole PMH array as overlapped, hence the homogeneous transformation matrix of body coordinate system $\{k\}$ relative to base coordinate system $\{0\}$ is:

$$T_{Hk} = \begin{bmatrix} 1 & 0 & (k-1)\cdot 2a \\ 0 & 1 & 0 \\ 0 & 0 & 1 \end{bmatrix} \tag{12}$$

Suppose the coordinate of any point in the base coordinate system $\{0\}$ is $(y_H, z_H)^T$. Then according to D-H conversion, the coordinate $(y_{Hk}, z_{Hk})^T$ of the point in the body coordinate system $\{\mathrm{k}\}$ can be calculated:

$$\begin{aligned} y_{Hk} &= y_H - 2a\cdot(k-1) \\ z_{Hk} &= z_H \end{aligned} \tag{13}$$

Substitute the expressed (11) and (13) into Formula (9) and (10). The magnetic field generated by PMH at Point $(y_{Hk}, z_{Hk})^T$ can be calculated:

$$\begin{aligned} B_{Hy} &= \sum_{k=1}^{n} f_y(a_k, y_{Hk}, z_{Hk}) \\ &= \sum_{k=1}^{n} f_y(a_0 + (k-1)\times Da, y_H - 2a\times(k-1), z_H) \end{aligned} \tag{14}$$

$$\begin{aligned} B_{Hz} &= \sum_{k=1}^{n} f_z(\alpha_k, y_{Hk}, z_{Hk}) \\ &= \sum_{k=1}^{n} f_z(\alpha_0 + (k-1)\cdot\Delta\alpha, y_H - 2a\cdot(k-1), z_H) \end{aligned} \tag{15}$$

2.5 Calculation of thrust and normal force

The structure of PMH&ILC type LSM is in Fig. 7.

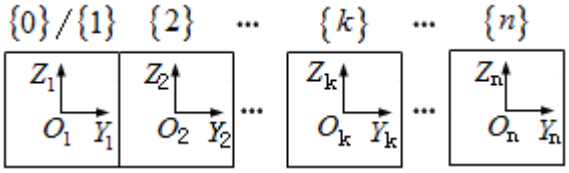

Fig. 7: Structure of PMH&ILC Type LSM

In ILC of motor secondary is three-phase alternating current electrified as shown in Figure 7. In one PMH cycle there are totally six cables named as No.$m\,(m=1,\cdots 6)$ cable. Then the coordinate of No.m cable is:

$$\begin{bmatrix} y_{0m} \\ z_{0m} \end{bmatrix} = \begin{bmatrix} y_0 + (m-1)\lambda/6 \\ z_0 \end{bmatrix}, z_0 = b + \delta + r \tag{16}$$

The phase sequence of three-phase alternating current in the cables can be obtained by unwinding rotating three-phase motor as shown in Fig. 8[23].

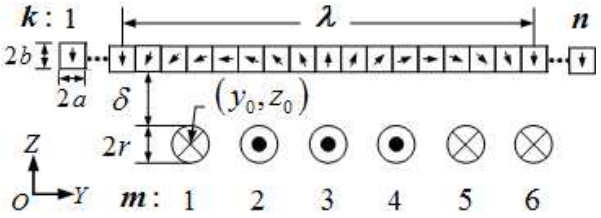

Fig. 8: Current in Three-Phase Motor Winding

Suppose the third cable in the figure is located right below permanent magnet segment with 0° in magnetization angle. Suppose its initial phase is 0, then the current in No.m cable at t moment is:

$$I_m = I_0\cdot\cos\left(\theta_t + \frac{m-3}{3}\pi\right), (\theta_t = \omega t) \in [0, 2\pi] \tag{17}$$

Here, ω represents angular frequency of current.

The magnetic force generated by the motor as shown in Figure 7 is sum of Ampere force borne by the six cables within single cycle. According to the method in Figure 6, the homogeneous transformation matrix from body coordinate system of permanent magnet segments to global coordinate system $\{0\}$ in Figure 7 is,

$$T_k = \begin{bmatrix} 1 & 0 & 2a\cdot(k-1) \\ 0 & 1 & 0 \\ 0 & 0 & 1 \end{bmatrix} \tag{18}$$

The coordinate of No.m cable in body coordinate system $\{k\}$ can be calculated:

$$\begin{aligned} y_{km} &= y_0 + (m-1)\,\lambda/6 - 2a\cdot(k-1) \\ z_{km} &= b+\delta+r \end{aligned} \tag{19}$$

Substitute (19) into (14) and (15), the $B_{ym}B_{ym}$ and B_{zm} are:

$$\begin{aligned} B_{ym} &= \sum_{k=1}^{n} f_y\left(\alpha_0 + (k-1)\cdot\Delta\alpha,\right. \\ &\left. y_0 + (m-1)\,\lambda/6 - 2a\cdot(k-1), b+\delta+r\right) \\ B_{zm} &= \sum_{k=1}^{n} f_y\left(\alpha_0 + (k-1)\cdot\Delta\alpha,\right. \\ &\left. y_0 + (m-1)\,\lambda/6 - 2a\cdot(k-1), b+\delta+r\right) \end{aligned} \tag{20}$$

Thus, the thrust and normal force generated by PMH&ILC type LSM are respectively,

$$F_y = \sum_{m=1}^{6} F_{ym} = \sum_{m=1}^{6} B_{zm}\cdot I_m \cdot L \tag{21}$$

$$F_z = \sum_{m=1}^{6} F_{zm} = \sum_{m=1}^{6} B_{ym}\cdot I_m \cdot L \tag{22}$$

Here, L represents width of the motor and I_m is determined by Formula (17).

3 Measurement of Motor Thrust

For a certain PMH&ILC type LSM motor, its related parameters are shown as follows: 180mm in electrode distance, 500mm in motor width, aluminum wire in primary coil, with 38.8 mm in outer diameter and 20.4 mm in aluminum core diameter, 45mm*45mm in section dimension of permanent magnet and permanent magnet material of NdFe48M. In the process of computation and measurement, the air-gap between the secondary and primary is 10mm. The photo of the synchronous linear motor is shown in Figure 9.

The working condition of test has been shown as in Fig. 10. As showed in Fig. 10, the pressure sensor is fixed on a mouting rack, and the mouting rack is fixed on the railway. The move direction of the secondary(PMH) is face to the mounting rack. When the thrust is generated, the PMH will press the pressure sensor. From the output of the pressure sensor, the thrust can be obtained. Electrify the primary(ILC) to current with different power angles, the thrust of motor can be tested. Draw the power angle property curve of the motor by tracing points.

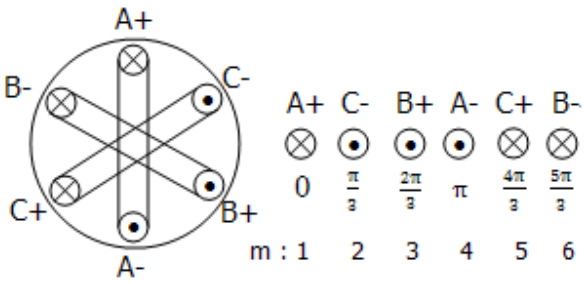

Fig. 9: PMH&ILC Type LSM Motor

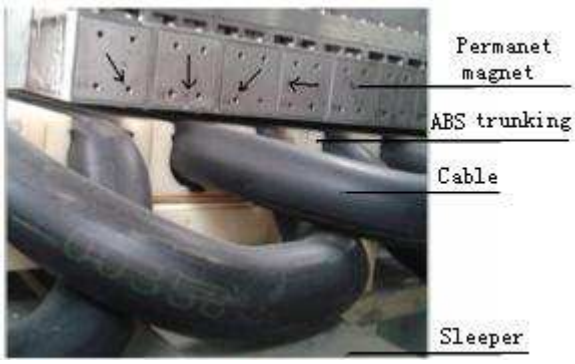

Fig. 10: Measurement for Motor Thrust

The value of direct current as stably outputted by the frequency convertor is the direct current amount of current peak 86A three-phase alternating current at different power angles after d-q axis conversion. The test result is seen in Table 1. The output of pressure sensor is voltage, in which 1V indicates 311kg of pressure.

Draw the measurement result of motor thrust in Table 1 and the calculation result of analytical expression into a curve. The result is seen in Fig. 11.

As only 1/4 cycle of values are measured, only 1/4 cycle of measurement curve is seen in curve chart 11.

From Figure 11, it can be seen that the motor thrust has very good consistency between the calculated value and the measured value. As the test motor is permanent magnet air-core linear motor without cogging force, and the secondary permanent magnets are in Halbach array with good sine degree of air-gap magnetic fields, the power angle property of thrust presents standard sine and the power angles corresponding to maximum thrust are

90°. It can also be seen that the maximum thrusts of the motor as tested and calculated are respectively 30.2 kg and 31.2 kg with 3.2% in error.

Table 1: Measurement Result of Motor Thrust

Power Angle (Degree)	Output of Sensor(V)	Thrust (kg)
12	0.007	2.177
27	0.032	9.952
42	0.056	17.416
57	0.074	23.014
72	0.087	27.057
82	0.093	28.923
87	0.095	29.545
88	0.094	29.234
89	0.096	29.856
90	0.097	30.167
91	0.095	29.545
92	0.094	29.234
102	0.093	28.923
117	0.083	25.813

Fig. 11: Measured and Calculated Value of Motor Thrust

4 Conclusion

This article studied the computation technology for the magnetic field and force of PMH&ILC-typed LSM. To calculate the magnetic field in the air-gap, the magnetic field produced by a single current-surface is derived from the equivalent surface-current model of a permanent magnet cubic, and then the magnetic field distribution of the whole PMH is deduced by D-H transform method. After introducing three-phase alternating current into ILC, the analytical solutions to the propulsion and normal forces of the motor are obtained. The validity of the proposed analytical solutions to the magnetic field in the air-gap and the forces generated by the motor is testified by experiment. It measures, with specific synchronous traction motor test platform, the actual thrust of the motor and makes comparison between the measured value and the calculated value. The comparison result indicates: the measurement result is basically consistent with the calculation result of the analytical calculation method. On account of small calculation, short calculation duration and convenient design, such analytical method has strong practicability in the initial stage of design of the permanent magnet linear synchronous motor.

The authors are grateful to the anonymous referee for a careful checking of the details and for helpful comments that improved this paper.

References

[1] Shoda Eisuke, Fujie Xunzhi, Kato Chunlang. Technology of Magnetically Levitated Vehicle [M]. Japan Ohmsha, Ltd, 1992
[2] Tang Renyuan. Modern Permanent Magnet Machines: Theory and Design. China Machine Press, 2008.
[3] Halbach K. Permanent Magnets for Production and Use of High Energy Beams[C]. Proceedings of the 8th International Workshop on Rare-earth Permanent Magnets, 1985: 123-136.
[4] Zhang Yong, Xu Shangang. Analysis of The Force And Field of Air-Core Permanent Magnet Linear Synchronous Motor [J]. Small & Special Electrical Machines. 1998, 25-27.
[5] Lu Qinfen. Research on characteristic of linear synchronous motor [D]. Hangzhou: Zhejiang University, 2005.
[6] Pang Hongshuai Research on characteristic of maglev linear synchronous motor [D]. Dalian: Dalian Jiaotong University, 2008.
[7] Qiu Lin. Magnetic field, performance analysis and optimization based on hereditary arithmetic of linear synchronous motor [D]. Shanghai: Shanghai University, 2003.
[8] Li Chengjun. Research on design and control strategy of maglev permanent magnet linear synchronous motor [D]. Shenyang: Shenyang Industry University, 2011.
[9] Hu Ganjun. Research on electromagnetic characteristic of maglev long-stator linear synchronous motor [D]. Hangzhou: Zhejiang University, 2005.
[10] Sun Peng, Zhou Huixing. Analysis and Experimental Research of Air-gap Magnetic Field of U-shaped Ironless Permanent Magnet Linear Synchronous Motor[J]. Micromotors, 2009, **42**: 9-12.
[11] Sam Gurol, Bob Baldi, Richard L. Post. Overview of the General Atomics Low Speed Urban Maglev Technology Development Program. Lausanne: Maglev'2002 Proceedings, 2002, 3: 8-16.
[12] Sam Gurol, Robert Baldi, Daryl Bever, Richard Post. Status of the General Atomics Low Speed Urban Maglev Technology Development Program. Shanghai: Maglev'2004 Proceedings, 2004, 269-274.
[13] D. Bruce Montgomery. Overview of the 2004 Magplane Design[C]. Shanghai: Maglev'2004 Proceedings, 2004, **1**: 106-112.

[14] Jiarong Fang, John Lawson, D. Bruce Montgomery. A New Pipeline System Transporting Coal Ores[C]. Daejeon: Maglev'2011 Proceedings, 2011, 200-205.
[15] Zhang Yong Xu Shangang. Analysis of The Force And Field of Air-Core Permanent Magnet Linear Synchronous Motor[J]. SMALL & SPECIAL MACHINES, 1998, 25-27.
[16] James F. Hoburg. Modeling Maglev Passenger Compartment Static Magnetic Fields From Linear Halbach Permanent-Magnet Arrays[J]. IEEE Transactions on Magnetics. 2004, **40**: 59-64.
[17] Z. P. Xia, Z. Q. Zhu and D. Howe. Analytical Magnetic Field Analysis of Halbach Magnetized Permanent-Magnet Machine[J]. IEEE Transactions on Magnetics. 2004, **40**: 1864-1872.
[18] Halbach K. Perturbation effect in segmented rare earth cobalt magnets [J]. Nuclear Instruments and Methods, 1982, **198**: 213-215.
[19] Zhu H Q, Xia Z P, Atallach, et al. Powder alignment system for anisotropic bonded NDFeB Halbach Cylinders [R]. 2000 IEEE, 0018-9464.
[20] Zhu Z Q, D. Howe. Halbach Permanent Magnet Machines and App lications2a Review [C]. Proc. Inst. Elect. Eng. Electric Power Applications, 2001, **148**: 299-308.
[21] Feng Cizhang. Electromagnetic Field [M]. Beijing: People's Education Press, 1980.
[22] Zhou Yuanqing, Zhang Zaixing. Intelligent Robot System [M]. Beijing: Tsinghua University Press, 1989.
[23] Authored by S. A. Nasar, I. Boldea. Translated by Long Xialing, Zhu Weiheng, Xu Shangang, Tian Lixing. Linear Motor [M]. Beijing: Science Press, 1982.

Hengkun Liu was born in Jangjin, Chongqing, China, in 1975. He received the PH.D degree in 2005works for National University of Defense Technology as a teacher. His research interests include control theory and its application, and maglev train levitation control technique.

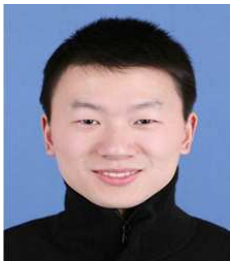

Hu Cheng was born in Xiangfan county, Hubei Province, China, in 1981. He received the PH.D degree in 2011works for National University of Defense Technology as a teacher. His research interests include control theory and its application, and maglev train levitation control technique.